An Enhanced Network Learning Method for Dynamic Probabilistic LCF Evaluation of Turbine Blisk

Cheng-Wei Fei
Department of Aeronautics and Astronautics
Fudan University
Shanghai, China
cwfei@fudan.edu.cn

Cheng Lu
School of Aeronautics
Northwestern Polytechnical University
Xi'an, China
lucheng2013@163.com

Wen-Zhong Tang
School of Computer Science and Technology
Beihang University
Beijing, China

***Abstract*—To reasonably predict the blisk LCF life, an enhanced network learning method (ENLM) was proposed by integrating neural network of regression with extremum thought. The developed ENLM was mathematically modeled and the method of reliability analysis with the ENLM were investigated. Then the LCF life reliability of a turbine blisk were evaluated utilizing the proposed ENLM by considering thermal-structural interaction and the stochastic characteristics of parameters. It is illustrated in the analysis to the reliability degree of blisk (0.998,5) and blisk LCF life (9,419 cycles) under the allowable value 6,000 cycles, which ensures some life margin for the blisk relative to the deterministic analysis. The comparison of methods reveals that the proposed ENLM has highly-computing efficiency and precision. The advantages of this method will more outstand with the increasing simulations. The outcome of this paper is to develop a promising tool for the reliability-based design optimization of gas turbine blisk LCF life in future work.**

Keywords-turbine blisk; LCF life; probabilistic analysis; ENLM; extremum response

I. INTRODUCTION

Turbine blisk is a core component of aeroengine heat-end and bearing extreme cyclic loads under high-temperature and high-speed operation. The low cycle fatigue (LCF) failure of blisk commonly appears owing to large easily-plastic deformation of blisk [1]. The randomness of parameters is key factors on the failure of blisk LCF [2]. For turbine blisk's safety and reliability, it is urgent to assess the reliability of blisk LCF life via a probabilistic investigation [3].

Under the study on the LCF life of structures widely, lots of methods have emerged comprising direct simulation method with Monte Carlo (MC) and surrogate model (or-called response surface method, RSM). Direct simulation method is a frequently-used approach [4-7]. This method is unworkable for thousands of iterations in the probabilistic LCF life analyses of structures, due to unacceptable computational loads and computational efficiency. With the advances of the theory and methods on structural reliability, many surrogate methods have been developed [8,9,10]. Zhang et al. proposed an extremum response surface method (ERSM) which can address the time-varying issue in the transient reliability evaluation of a flexible mechanism [11]; Lu et al. discussed an improved surrogate method based on Kriging model and ERSM for multi-failure probabilistic analyses of structures [12]. The works in [11,12] revealed that ERSM can precisely and efficiently handle the transient probabilistic analysis problem for the reliability-based LCF life analysis of turbine blisk under aeroengine operation. For another, it is difficult for the ERSM to satisfy the requirement of precision, for the weakness in nonlinear probabilistic analyses.

A generalized regression neural network (GRNN) was developed from neural network technology to efficiently resolve the nonlinear problem, because it holds strong nonlinear mapping and good robustness [13]. Li et al. derived the prediction model of power loads introducing the drosophila optimization algorithm into the GRNN with a strong nonlinear model capability [14]. Sun et al. demonstrated the superiority of the GRNN model in terms of computational precision and efficiency compared with the back propagation neural network (BPNN) model [15]. Wang et al. explored the application of the GRNN in the source localization of underwater ocean waveguides [16]. Therefore, the GRNN method is highly accurate and businesslike.

To enhance the modelling accuracy and simulation efficiency in turbine blisk LCF life reliability analysis, an enhanced network learning method (ENLM) is proposed in respect of ERSM with the ability of dynamic processing and GRNN with the advantages of small samples and nonlinear mapping. The reliability-based LCF life estimation of turbine blisk is accomplished with the proposed method, with regard to random input variables and minimum fatigue life. The effectiveness of the developed ENLM is verified by comprising with other methods (i.e., MCM and ERSM).

II. BASIC THEORY

A. Low Cycle Fatigue Life Modelling

In engineering, Mason-Coffin equation is always adopted to express the relationship between strain and fatigue life [17], i.e.,

978-1-7281-0860-5/19/$31.00 ©2019 IEEE

$$\frac{\Delta\varepsilon}{2}=\frac{\sigma_f^{'}}{E}\left(2N_f\right)^b+\varepsilon_f^{'}\left(2N_f\right)^c \tag{1}$$

where $\Delta\varepsilon$, E, $\sigma_f^{'}$ and $\varepsilon_f^{'}$ indicate the sum of specified material strain, the elasticity modulus of material, the coefficient of fatigue strength and the coefficient of fatigue ductility, respectively; b and c are fatigue strength exponent and fatigue ductility exponent, respectively; N_f expresses low cycle fatigue life.

In respect of the mean stress σ_m produced by complicated loadings under aeroengine run, based on the Ref.[18] the formula (1) can be derived as

$$\frac{\Delta\varepsilon}{2}=\frac{\sigma_f^{'}-\sigma_m}{E}\left(2N_f\right)^b+\varepsilon_f^{'}\left(2N_f\right)^c \tag{2}$$

The LCF life is determined considering the Miner law and the effect of cyclic loads, i.e., the fatigue damage D is

$$D=\sum_{i=1}^{r}\frac{n_i}{N_i} \tag{3}$$

here r indicates the number of loading levels; N_i denotes fatigue life for ith loading level; n_i is cyclic number for ith loading level.

B. Extremum Response Surface Modeling

To handle the dynamic characteristics of workloads and the nonlinearity of input parameters, the ERSM was proposed in [11] to transform the output process of LCF life into a minimum in an analytical time domain. Assuming $\boldsymbol{X}$ and y_e are input variables set and extremum output response, the model of ERSM $y_e(\boldsymbol{X})$ [11] is expressed as

$$f\left(X\right)=y_e\left(X\right)=\left\{y_e^{(j)}X^{(j)}\right\} \tag{4}$$

in which $X^{(j)}$ stands for the jth set of input samples; $y_e^{(j)}X^{(j)}$ indicates the extreme value of output response in time domain.

ERSM models were traditionally derived on basis of quadric polynomials [12], and these models were usually inefficient and inaccurate in modelling, the reason is that the quadric polynomials and the least square method are unsuitable for multi-variable and high-nonlinear problems. We thus fused the superiorities of the GRNN method (strong nonlinear mapping ability and good robustness) and ERSM to improve analytical precision and computational efficiency.

C. Mathematical Model of Enhanced Network Learning Method

ENLM is a feedforward network model with the theory of nonlinear regression, which comprises input layer, hidden layer and output layer. The structure of ENLM is shown in Figure 1.

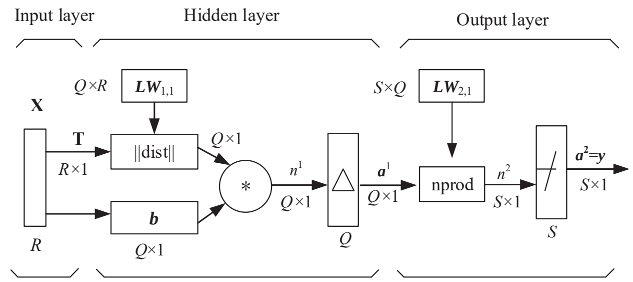

***Note**:* $\boldsymbol{X}$—input samples matrix; $\boldsymbol{T}$—output samples matrix; $Q\times R$—the dimensions of matrix $\boldsymbol{LW}_{1.1}$ which is the weighted matrix in hide layer, where Q and R are the number of training samples and input parameters, respectively; ||dist||—Euclidean distance function; $\boldsymbol{b}$—the threshold of Q neural cells in hidden layer; n^1—the network vector of hide layer; △—transfer (Gauss) function; $\boldsymbol{a}^1$—the output of neuro cell; $S\times Q$—the dimensions of matrix $\boldsymbol{LW}_{2.1}$ which is connection threshold value between hide layer and output layer, where S is the number of output parameters; nprod—the weight function of output layer; n^2–the network vector of output layer; ⁄—the purelin transfer function of output layer; $\boldsymbol{y}$=a^2—the outputs of neuro cell in output layer.

Figure 1 Structure of enhanced network learning method

As for the input layer, the input output matrixes with training samples, $\boldsymbol{X}$ and $\boldsymbol{T}$, are

$$\boldsymbol{X}=\begin{bmatrix} x_{11} & x_{12} & \cdots & x_{1Q} \\ x_{21} & x_{22} & \cdots & x_{2Q} \\ \cdots & \cdots & \cdots & \cdots \\ x_{R1} & x_{R2} & \cdots & x_{RQ} \end{bmatrix},\ \boldsymbol{T}=\begin{bmatrix} t_{11} & t_{12} & \cdots & t_{1Q} \\ t_{21} & t_{22} & \cdots & t_{2Q} \\ \cdots & \cdots & \cdots & \cdots \\ t_{S1} & t_{S2} & \cdots & t_{SQ} \end{bmatrix} \tag{5}$$

in which x_{ji} (j=1,2, …, R; i=1,2, …, Q) indicates jth input sample against ith training samples; t_{ji} denotes jth output sample to ith training samples; R is the number of input variables; S represents the number of outputs; Q indicates the number of training samples.

The neurons in hidden layer was the number of training samples and weight function can be expressed by Euclidean distance function, thus weight matrix in implicit layer is

$$\boldsymbol{LW}_{1,1}=\boldsymbol{X}^T \tag{6}$$

The thresholds $\boldsymbol{b}$ of Q neural cells in hidden layer, i.e.,

$$\boldsymbol{b}=\left[b_1,b_2,\cdots b_Q\right]^T \tag{7}$$

in which b_1=b_2=…=b_Q=0.8326/σ where σ illustrates the smooth factor of Gauss function.

Gaussian radial basis function is usually adopted as the transfer function of hidden layer. In hidden layer, the number of neurons Q and training samples is the same, and one training sample has a neuron. Based on the values of weight matrix and thresholds, the output a_i^j of ith hidden layer neuron is

$$a_i^j=exp\left(-\frac{0.8326\left\|\boldsymbol{LW}_{1,i}-\boldsymbol{x}_j\right\|^2}{\sigma}\right) \tag{8}$$

in which $\boldsymbol{LW}_{1,i}$=[x_{h1}, x_{h2}, …, x_{hR}]^T subject to h=1,2, …, Q indicates the vector of ith implicit layer in $\boldsymbol{LW}_{1,1}$; $\boldsymbol{x}_j$=[x_{j1}, x_{j2}, …,

$x_{jR}]^T$ is jth training samples vector. $a^j = \left[a_1^j, \cdots, a_i^j, \cdots a_Q^j\right]$ is Q nerve cells vector for jth input samples.

Regarding the $\boldsymbol{LW}_{2,1}$ as the output matrix of training samples set, i.e.,

$$\boldsymbol{LW}_{2,1}=\boldsymbol{T} \tag{9}$$

and the third layer of GRNN as the output layer, in respect of (8) and (9) the vector n^j is

$$n^j = \frac{\boldsymbol{LW}_{2,1}\left[\boldsymbol{a}^j\right]^T}{\sum_{i=1}^{Q} a_i^j} \tag{10}$$

Regarding the line transfer function $y^j=purelin(n^j)$ of n^j, the GRNN model subject to the response of jth training samples is

$$y^j = \text{purelin}\left(n^j\right) = \frac{\boldsymbol{LW}_{2,1}\left[\boldsymbol{a}^j\right]^T}{\sum_{i=1}^{Q} a_i^j} \tag{11}$$

Combined with (4), the ENLM model is

$$y_{min}^j = Min\left\{\frac{\boldsymbol{LW}_{2,1}\left[\boldsymbol{a}^j\right]^T}{\sum_{i=1}^{Q} a_i^j}\right\} \tag{12}$$

D. Reliability Analysis Approach with ENLM Model

When y^* and y_{min}^j indicate the allowable values of LCF life and fatigue life function, the limit state function of structural LCF life is [19]

$$Z=y_{min}^i - y^* \tag{13}$$

here Z>0 explains the safe blisk structure, and vice versa. When random input variables are mutually independent and obey normal distributions, the output response of LCF life distributes normally. Hence the reliability degree P_r [19] is

$$P_r = \Phi\left(\frac{\mu_Z}{\sqrt{D_Z}}\right) \tag{14}$$

where μ_z and D_z are the mean and variance of Z.

Considering thermal-structure coupling, the procedures of the reliability-based LCF life analysis of turbine blisk with the ENLM are described below.

Step 1: Generate the finite element (FE) model based on the three-dimension model of blisk.

Step 2: Set boundary conditions in view of the numerical features of random inputs, perform the deterministic analysis with the blisk FE model, and then determine the design point with the minimum fatigue.

Step 3: Obtain a handful of input samples by adopting Latin hypercube sampling(LHS) method [21] and the LCF life values of turbine blisk, and ensure a training sample set.

Step 4: Train the ENLM model by using the cross-validation method to define radial basis function, connection weights and optimal smooth factors [20].

Step 5: Structure the limit state function of blisk LCF life based on the ENLM model build.

Step 6: Verify the precision of ENLM model. If satisfied, implement ***Step 7***; conversely, return to ***Step 4***.

Step 7: Determine reliability degree based on the reliability-based LCF life analysis of turbine blisk with thermal-structure coupling, by extracting enough samples with the MC method.

III. PROBABLISTIC LOW CYCLE FATIGUE LIFE ANALYSES OF TURBINE BLISK

A. Random Variables

We selected an aeroengine high-pressure turbine blisk made by GH4133 as the study object in this work. For the blisk LCF life design and prediction, the related parameters have uncertainties. The random features of input variables are reasonably determined according to engineering practice and previous experience, which include gas temperature T, rotor speed ω, elasticity modulus E, material density ρ, heat conductivity λ, fatigue ductility coefficient ε'_f, fatigue strength efficient σ'_f, fatigue ductility index c and fatigue strength index b. The distribution features of the variables are listed in TABLE Ⅰ.

TABLE I. DISTRIBUTIONS OF RANDOM VARIABLES

Random Variables	Mean μ	Std. Dev. δ	Distribution
ρ	8,210 kg.m^{-3}	328.4 kg.m^{-3}	Normal
E	163,000 MPa	4,890 MPa	Normal
λ,	23 W·m^{-1}·°C^{-1}	0.005 W·m^{-1}·°C^{-1}	Normal
ω,	1,168 rad·s^{-1}	35 rad·s^{-1}	Normal
T_a,	1,173.15 K	35.2 K	Normal
T_b, k	1,473.15 K	47 K	Normal
σ'_f	1,419	42.5	Normal
ε'_f	50.5	1.53	Normal
b	−0.1	0.005	Normal
c	−0.84	0.042	Normal

B. Deterministic LCF Life Analysis of Turbine Blisk

The deterministic analysis of the turbine blisk was completed considering the thermal-structural interaction. Due to symmetry, 1/40 of the whole blisk was analyzed to lighten the burden of the calculation. The FE models (with 31,380 nodes and 17,111 elements) are shown in Figure 2a. The deterministic LCF life analysis of turbine blisk was finished following the input variables in TABLE Ⅰ. In the light of the Mason-Coffin damage rule in (2) and (3), the fatigue life values of the turbine blisk at the design point are shown in Figure 2b. As illustrated in Fig. 2b, the minimum fatigue life was 8,900.6 cycles. The LCF of the blisk should be about 4,450 cycles owing to the double safety coefficients in engineering.

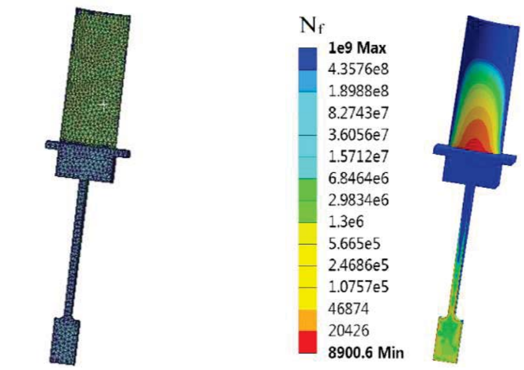

(a) FE gridding (b) Fatigue life

Figure 2 Gridding and fatigue life nephogram of turbine blisk

C. Low Cycle Fatigue Life Models of Turbine Blisk with ENLM

In line with the distribution of input random parameters in TABLE Ⅰ, 150 samples were extracted by LHS technology. And then the minimum LCF life was computed corresponding the input samples. 120 groups of samples were treated as the training set and the remaining samples (30 groups) were regarded as the testing set. These samples data are normalized. By the cross-validation method, the data were normalized for ENLM modeling by gaining the coefficients of ENLM, i.e., $\boldsymbol{b}$ and $\boldsymbol{LW}_{1,1}$and $\boldsymbol{LW}_{1,2}$ listed in (15). Therefore, the ENLM model can be derived with the determined parameters. Testing the established ENLM model was conducted by the rest 30 samples. The testing results are displayed in Figure. 3. As seen in Figure 3, the predicted data are almost the same to the true data, and the developed ENLM model holds a high prediction precision.

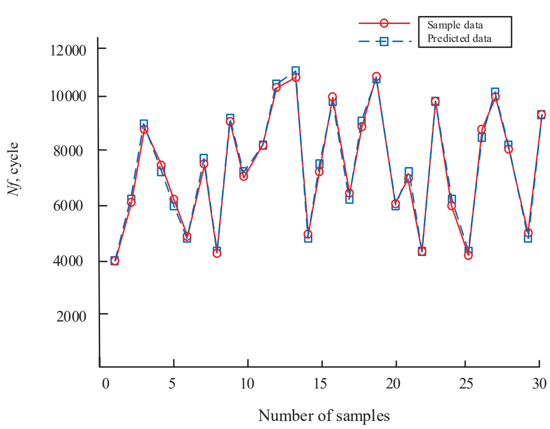

Figure 3 Test results of ENLM model with 30 samples

$$\begin{cases} \boldsymbol{LW}_{1,1} = \begin{bmatrix} -0.4189 & 0.0946 & \cdots & 0.9459 & 0.7972 \\ -0.8912 & -0.5646 & \cdots & -0.2517 & -0.1020 \\ 1.0000 & -0.5646 & \cdots & 0.7959 & -0.5510 \\ -0.7852 & -0.7315 & \cdots & -0.1678 & 0.4765 \\ 0.2245 & -0.8639 & \cdots & -0.6190 & -0.3878 \\ 0.5839 & 0.3020 & \cdots & 1.0000 & -0.7315 \\ 0.6510 & 0.2752 & \cdots & 0.1678 & -0.5973 \\ -0.6892 & 0.8514 & \cdots & -0.9865 & -0.4865 \\ -0.0470 & -0.5302 & \cdots & 0.6107 & 0.0366 \\ -0.1757 & -0.8108 & \cdots & 0.2838 & -0.3919 \end{bmatrix}^{T}_{10\times 120} \\ \boldsymbol{LW}_{2,1} = \begin{bmatrix} -0.9061 & -0.8701 & \cdots & -0.9968 & -0.9400 \end{bmatrix}_{1\times 120} \\ \boldsymbol{b} = \begin{bmatrix} 2.8710 & 2.8710 & \cdots & 2.8710 & 2.8710 \end{bmatrix}^{T}_{1\times 120} \end{cases} \quad (15)$$

D. Reliability-Based Low Cycle Fatigue Life Analysis of Turbine Blisk with the ENLM

The ENLM model was employed to perform the reliability-based LCF life analysis of the blisk by running 10,000 MC simulations. The analytical results of blisk LCF life involving historical simulation diagram and histogram are displayed in Figure 4. As found in Figure 4, the minimum fatigue life of the blisk distributes normally, the mean and standard deviation of which are 9419 life cycles and 967 life cycles, respectively. When the allowable fatigue life y^* of turbine blisk is 6 000 life cycles, the reliability degree P_r of LCF life is 0.998 5 computed by (13) and (14). The value of derived reliability degree satisfied with blisk strength design according to engineering experience. Meanwhile, the blisk fatigue life is 6 000 life cycles. However, with respect to the FE analysis, the minimum blisk LCF life is 8 900.6 life cycles in Fig. 4d. Regarding double safe coefficients, blisk safe fatigue life is about 4 450 life cycles in term of the deterministic analysis. Subsequently, it is shown that deterministic method is small relative to about 4 450 life cycles acquired in the probabilistic LCF life estimation of blisk at 6 000 life cycles, thanks to 4 450 life cycles smaller than 6 000 life cycles.

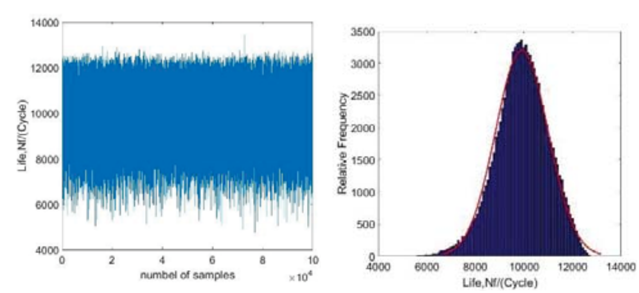

(a) Simulation history (b) Histogram

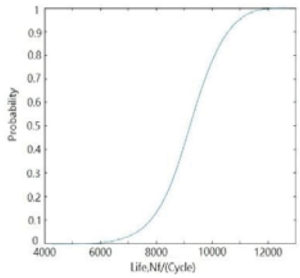

(c) Accumulative curve

Figure 4 Reliability-based LCF life results of blisk with ENLM

E. Validation of ENLM

To demonstrate the feasibility of the ENLM, adopting MC method and ERSM performs the reliability LCF life analyses of turbine blisk under different the numbers of simulations by adopting the same simulation environment. The computing time and reliability degrees are shown in TABLE Ⅱ and TABLE Ⅲ. In TABLE II and TABLE III, the precision for the method D_p was

$$D_p = 1 - \frac{|\gamma_a - \gamma_m|}{\gamma_a} \times 100\% \tag{16}$$

TABLE II. COST TIME OF ENLM, MC SIMULATION METHOD AND ERSM

Number of Samples	Cost Time for Simulations, s			Reduced Time, s	Improved Efficiency, %
	MC Method	*ERSM*	*ENLM*		
10^2	5,400	1.249	1.201	0.048	3.843
10^3	14,400	1.266	1.201	0.065	5.134
10^4	432,000	1.681	1.311	0.370	15.18
10^5	—	2.437	1.342	1.095	44.93
10^6	—	4.312	2.138	2.174	50.42

TABLE III. COMPUTING ACCURACY OF METHODS FOR MANY NUMBERS OF SIMULATIONS

Samples	Degrees of Reliability			Precision, %		Improved Precision, %
	MC	*ERSM*	*ENLM*	*ERSM*	*ENLM*	
10^2	0.85	0.76	0.79	76.24	79.25	3.01
10^3	0.976	0.947	0.968	95.00	97.11	2.11
10^4	0.9968	0.9824	0.9973	98.56	99.95	1.39
10^5	—	0.98181	0.99848	98.49	99.83	1.34
10^6	—	0.98262	0.99587	98.58	99.91	1.33

As seen in TABLE Ⅱ, as simulations increases, the consumption time rises for these three methods. When the simulations larger than 10,000, the MC method requires an excessive computational burden and even unable to accomplish the computational task. However, the ERSM and ENLM can implement the number of simulations from 100 to 1,000,000 with a few seconds. In addition, the developed ENLM spends few time and is high-efficient by comparison of the ERSM, and the superiority of the ENLM is more remarkable with the rising simulations. At 10,000 simulations, for instance, the ENLM saves computing time 0.048 s and enhances simulation speed by 3.843% with respect to the ERSM, as well as reduces the computing time by 2.138 s and improves the computing efficiency by 50.42%. Therefore, it is illustrated that the presented ENLM processes strong computational ability and is highly-efficient in reliability-based simulations. Furthermore, high efficiency will be stronger with the largamente of simulations.

In TABLE Ⅲ, the reliability degree determined with the 10,000 MC simulations are treated as a datum point. In this case, we discover that the reliability degrees of ENLM and ERSM are 0.9923 and 0.9824 respectively, and the computing precisions of ENLM and ERSM are 99.95%and 98.56% , respectively. Additionally, the increase of turbine blisk's reliability degree with simulations based on the developed ENLM is more accurate than ERSM.

Therefore, the developed ENLM is highly-precise and -efficient, and the superiorities is more obvious as enlarge simulations.

IV. CONCLUSIONS

To improve the reliability and performance of turbine blisk, this paper proposed an enhanced network learning method (ENLM) for the reliability-based LCF life analyses of turbine blisk, b absorbing the nonlinear mapping and small sample-based modeling superiorities of regression neural network and the transient processing of extremum method. Through this study, it is revealed that the LCF life reliability degree of the blisk is about 0.998,5 when the allowable value was 6,000 cycles determined by engineering experience, and the design had enough margin of approximately 1550 cycles to ensure the normal operation of aeroengine. Through the comparison of different methods, it is fully illustrated that the developed ENLM holds higher modeling precision and computing efficiency relative to MC method and ERSM. Moreover, the outstanding of ENLM enlarges with the rise of simulations. The efforts of this paper offer a promising approach for structural dynamic reliability analysis.

ACKNOWLEDGMENT

This research was funded by National Natural Science Foundation of China, grant numbers 51975024, 51475025and 51875465, Start-up Research Funding of Fudan University, grant number FDU38341, Innovation Foundation for Doctor Dissertation of Northwestern Polytechnical University, grant number CX201932. The authors would like to thank them.

REFERENCES

[1] H.F.Gao, A.Wang, G.C. Bai, Wei, C.M. and C.W. Fei, "Substructure-based distributed collaborative probabilistic analysis method for low-cycle fatigue damage assessment of turbine blade-disk," Aerosp. Sci. Technol., vol. 79, pp. 636–646, 2018.

[2] O. Scott-Emuakpor, T. George, C. Cross, and M.Shen, "Multi-axial fatigue-life prediction via a strain-energy method," AIAA J., vol. 48, pp. 63–72, 2010.

[3] S.P. Zhu, H.Z. Huang, R. Smith, V.Ontiveros, L.P. He, and M. Modarres, "Bayesian framework for probabilistic low cycle fatigue life prediction and uncertainty modeling of aircraft turbine disk alloys," Probab. Eng. Mech., vol. 34, pp. 114–122, 2013.

[4] Y. Sun, and L.S. Hu, "Low cycle fatigue life prediction of a 300MW steam turbine rotor using a new nonlinear accumulation approach," Proceedings of the 24th Chinese Control and Decision Conference (CCDC), Taiyuan, China, pp. 3913–3918, May 2012.

[5] T. Letcher, M.H.H. Shen, O. Scott-Emuakpor, T. George, and C. Cross, "An energy-based critical fatigue life prediction method for AL6061-T6," Fatigue Fract. Eng. Mater. Struct., vol. *35*, pp. 861–870, 2012.

[6] H. Bargmann, I. Rüstenberg, and J. Devlukia, "Reliability of metal components in fatigue: A simple algorithm for the exact solution," Fatigue Fract. Eng. Mater. Struct., vol. 17, pp. 1445–1457, 2010.

[7] S.P. Zhu, S. Foletti, and S. Beretta, "Probabilistic framework for multiaxial LCF assessment under material variability," *Int. J. Fatigue*, vol. 103, pp. 371–385, 2017.

[8] Fei, C.W.; Bai, G.C.; Tian, C. Extremum response surface method for casing radial deformation probabilistic analysis. *Aerosp. Inf. Syst.* 2013, 10, 47–52.

[9] G.C. Bai, and C.W. Fei, "Distributed collaborative response surface method for mechanical dynamic assembly reliability design," Chin. J. Mech. Eng., vol. 26, pp. 1160–1168, 2013.

[10] J.E. Hurtado, and D.A. Alvarez, "An optimization method for learning statistical classifiers in structural reliability," Probab. Eng. Mech., vol. 25, pp. 26–34, 2010.

[11] C.Y. Zhang, and G.C.Bai, "Extremum response surface method of reliability analysis on two-link flexible robot manipulator," J. Cent. South Univ., vol. 19, pp. 101–107, 2012.

[12] C. Lu, Y.W. Feng, R.P. Liem, and C.W. Fei, "Improved kriging with extremum response surface method for structural dynamic reliability and sensitivity analyses," Aerosp. Sci. Technol., vol. 76, pp. 164–175, 2018.

[13] K. Nose-Filho, A.D.P. Lotufo, and C.R. Minussi, "Short-term multinodal load forecasting using a modified general regression neural network," IEEE Trans. Power Deliv., vol. 26, pp. 2862–2869, 2011.

[14] H.Z. Li, S. Guo, C.J. Li, and J.Q. Sun, "A hybrid annual power load forecasting model based on generalized regression neural network with fruit fly optimization algorithm," Knowl. Based Syst., vol. 37, pp. 378–387, 2013.

[15] G. Sun, S.J. Hoff, B.C. Zelle, and M.A. Smith, "Development and comparison of backpropagation and generalized regression neural network models to predict diurnal and seasonal gas and PM 10 concentrations and emissions from swine buildings," Trans. Asabe., vol. 51, pp. 685–694, 2008.

[16] Y. Wang, and H. Peng, "Underwater acoustic source localization using generalized regression neural network," J. Acoust. Soc. Am., vol. 143, pp. 2321–2331, 2018.

[17] H. Gao, C. Fei, G. Bai, and L. Ding, "Reliability-based low-cycle fatigue damage analysis for turbine blade with thermo-structural interaction," Aerosp. Sci. Technol., vol. 49, pp. 289–300, 2016.

[18] C.L. Liu, Z.Z. Lu, Y.L. Xu, and Z.F. Yue, "Reliability analysis for low cycle fatigue life of the aeronautical engine turbine disc structure under random environment," Mater. Sci. Eng. A, vol. 395, pp. 218–225, 2005.

[19] C.W. Fei, W.Z. Tang, G.C. Bai, and M. Shuang, "Dynamic probabilistic design for blade deformation with SVM-ERSM," Aircr. Eng. Aerosp. Technol., vol. 87, pp. 312–321, 2015.

[20] Z. Wei, F. Feng, and W. Wei, "Non-linear partial least squares response surface method for structural reliability analysis" Reliab. Eng. Syst. Saf., vol. 161, pp. 69–77, 2017.

[21] X. Zhai, C.W. Fei, J.J. Wang, and Y.S. Choy, "A stochastic model updating strategy-based improved response surface model and advanced Monte Carlo simulation," Mech. Syst. Signal Pr., vol. 82, pp. 323-338, 2017.